RESEARCH ON LASER PROTECTION AT THE FRAUNHOFER IOSB

Gunnar Ritt[(1)], Dominik Walter, Bernd Eberle

Fraunhofer Institute of Optronics, System Technologies and Image Exploitation IOSB, Gutleuthausstrasse 1, 76275 Ettlingen, Germany

[(1)]Email: gunnar.ritt@iosb.fraunhofer.de

KEYWORDS: Laser dazzling, laser damage, sensor protection

ABSTRACT:

Since the invention of the laser in 1960, the protection of human eyes and sensors against dazzle and damage by laser radiation is a hot research topic. As long as the parameters of a laser source (e.g., the wavelength) are known, adequate laser safety can be ensured by utilizing conventional laser protection filters. This is typically the case in cooperative environments like a laboratory. A very different situation prevails in military defence or civil security. There, the parameters of a threatening laser are usually unknown.

Here, we present an overview of the research on laser protection at the Fraunhofer IOSB comprising measures against laser damaging and laser dazzling.

1. INTRODUCTION

Current laser protection measures are typically realized using conventional optical filters based on absorption, reflection or interference effects. However, these devices work only in a limited wavelength range and they introduce a strong colour distortion if they are designed for the visible spectral range. These restrictions do not pose a particular problem in well-known environments like a laboratory or an industrial facility, where all parameters of the laser sources in use are known. This situation does not apply to laser attacks on military troops or on civil safety authorities. There, the laser parameters are usually unknown, creating a demand for wavelength independent laser protection measures.

Originally, the research on broadband laser protection was driven by military needs in consequence of the development of anti-sensor laser systems [1,2]. These kinds of weapons were designed as pulsed laser sources based on nanosecond pulses. To counter them, protection devices must be capable to attenuate each single laser pulse on a timescale shorter than that of the threatening pulse. This specific problem excludes all kinds of active protection measures. The hot candidates in mind were so-called optical power limiters (OPL): devices showing a reduced transmittance for high input intensities, while providing high linear transmittance for low input intensities. Since the beginning of the 1980s, optical power limiters are an ongoing research topic.

Military anti-sensor laser weapons as mentioned above were available only in limited numbers distributed among a few nations. They are no longer the main laser threat to be faced by the troops. These days, an increasing threat for the military as well as for civil safety authorities originates from handheld laser pointers: battery-powered devices which are freely available and have a high distribution due to their rather low price. They are offered with output powers in the range of some milliwatts up to more than 1 W; a large variety of different wavelengths in the visible spectral region is available. Typically, these lasers do not work as pulsed sources but emit continuous wave (cw) radiation. In contrast to the above-mentioned military pulsed laser systems, active laser protection measures are a possible solution for this threat.

The ideal protection measure, capable to counter laser dazzling and damaging, should fulfil various requirements, including:

1. Protection covering the complete operating spectral range of the sensor/human eye with the ability to protect against a number of different wavelengths at the same time.

2. Sufficient attenuation of laser light, while offering a high transmittance for non-hazardous radiation.
3. No colour distortion for the human eye or sensors working in the visible spectral region.
4. Acting only on parts of the field of view where harmful radiation occurs, whereas not affecting those parts where no laser light is present.
5. Protection against monochromatic laser sources (both cw and pulsed) as well as broadband light sources (e.g., the sun or high-power LEDs).
6. Realizable as a thin film that can be put, for example, on existing optics or windshields.

Numerous kinds of approaches were discussed in literature regarding concepts for laser protection. A short review of several techniques is given by SVENSSON and co-workers [3]. They distinguish three types of protection measures: (a) static protection, (b) active protection and (c) self-activating protection. Static protection measures, such as fixed line filters, offer a very high attenuation but exhibit several disadvantages (e.g., limited working wavelength range). Active systems suffer from the disadvantage of a finite response time. They are useful for the protection against continuous wave laser sources or repetitive laser pulses but they are not able to protect against single laser pulses. In this case, a self-activating protection (e.g., optical power limiters) seems to be the most promising technology. Unfortunately, the maximum attenuation of these devices is still too low to ensure adequate protection. In summary, none of the protection technologies available today is able to fulfill all the requirements stated before. An all-embracing solution is still far out of reach.

At the Fraunhofer IOSB in Ettlingen, Germany, formerly known as FGAN-FfO (until 1999) and FGAN-FOM (1999–2009), research on laser protection has been performed for more than two decades. The early work was focused on the protection of thermal imagers against laser radiation. Reversible and irreversible effects of intense laser radiation on thermal imagers (including the assessment of damage thresholds) were studied intensively. The optical nonlinearities of various materials were examined as possible protection measure against laser radiation. In the late 1990s, the protection against laser radiation in the visible/near-infrared spectral region took on greater significance.

In this paper we present an overview of the past and current work on laser protection at our institute. The subjects will not stick to a chronological order but rather to a content-related order. Section 2 starts with the evaluation of laser threats. It comprises the results of studies on reversible and irreversible effects of intense laser radiation on electro-optical sensors and some (basic) theoretical calculations. Section 3 summarizes the research on optical power limiting both for the infrared and visible spectral region and is related to the protection of electro-optical sensors and the human eye against damaging by laser radiation. From the plenty of our investigations, we will mainly discuss this topic by introducing two selected examples relating to the older work in the LWIR and to current work in the visible. Section 4 presents an electro-optical sensor hardened against dazzling by continuous wave laser sources as a measure against the increasing threat of high-power laser pointers.

2. LASER THREAT ANALYSIS

Research on laser protection measures is not only focused on protection measures against dazzling and damaging itself. It also includes the analysis of possible threats and the impact of these threats on the objects to be protected. Damaging may be regarded as the worst case since the resulting disturbance is irreversible. Single laser pulses may already cause a severe reduction of performance. Dazzling relates to reversible effects induced by either high repetition laser pulses or continuous wave lasers. Although these effects are reversible, the impact on missions can be critical. In the case of the human eye, the different levels of impairment ranging from dazzling to damaging are characterized by their physiological impact. The suppression of these effects depends on the given scenario. Giving an example, section 2.1 discusses the levels of protection necessary to counter specific threats.

2.1 Theoretical considerations

One of the most important parameters for a potential laser protection measure is the maximum attainable attenuation. Fig. 2-1 gives an example for

the necessary levels of attenuation regarding the respective physiological effects. Both intraocular power and corneal irradiance are plotted as a function of the distance of an observer's eye to the exit port of a laser source.

Threshold values for eye damage and various types of dazzling effects are indicated in the graph by horizontal lines. The highest value is the so-called maximum permissible exposure (MPE), which indicates the level for eye damage [4]. This value depends on several parameters like the laser wavelength or duration of exposure. The three lower lines show the visual interference levels according to [5]: 100 µW/cm² ("significant flash blindness"), 5 µW/cm² ("significant glare") and 50 nW/cm² (no distraction).

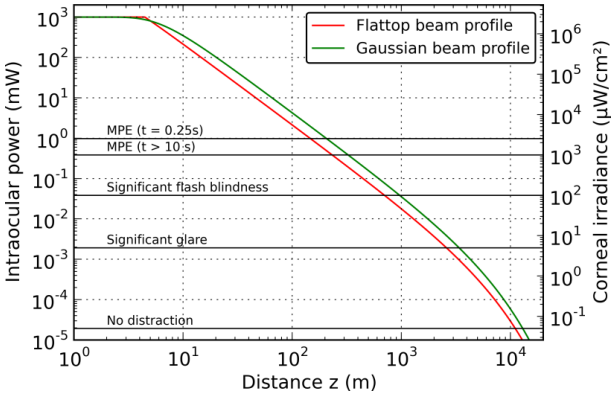

Figure 2-1. Intraocular power and corneal irradiance as a function of the distance to the laser source. Assumed calculation parameters as described in the text.

For the calculations, we assume following laser parameters: Power P = 1 W; beam diameter at the exit port d_0 = 2 mm; full angle divergence Φ = 1.5 mrad; wavelength λ = 532 nm. These values correspond to handheld laser devices that can be purchased on the free market. The diameter of the eye pupil was assumed to be 7 mm. The calculations were performed for both a flattop beam profile and a Gaussian beam profile and an atmospheric extinction of 0.2 km-1 (good visibility).

From the graph, we can deduce that attenuation in power of at least three orders of magnitude is necessary to stay below the MPE at all distances to the laser source. Dazzling effects occur already about four orders of magnitude below the MPE. Thus, even higher attenuations are required, in order to protect the eye against dazzling too (more than seven orders of magnitude to prevent from distraction in the case assumed).

2.2. Effects of laser irradiation on infrared cameras – damaging and dazzling

Damaging:

First measurements at the institute regarding the damage threshold of thermal imagers were conducted in 1994. A backside-illuminated CMT detector (the backside is facing the incoming laser radiation) was irradiated with pulses of a CO_2 laser source (LSI PSL 300, λ = 10.6 µm, pulse width of the gain switch spike: 200 ns). To identify the laser damage threshold, the pulse energy was gradually increased and the responsivity of the examined detector element was measured before and after the laser exposure. The damage threshold was measured for single pulses as well as for pulse series. Fig. 2-2a shows the responsivity of the detector as a function of the fluence; the abrupt decrease of the responsivity is clearly observable.

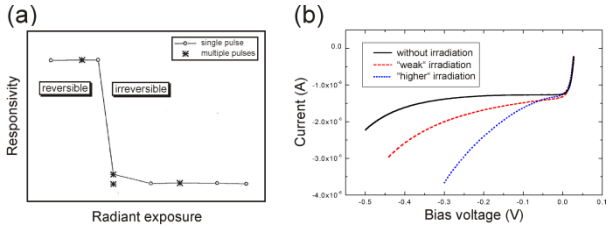

Figure 2-2.(a) Responsivity of a CMT detector as a function of the fluence for single pulse (circles) and multiple pulse (stars) irradiation. (b) Change of the diode characteristic of a CMT detector after the impingement with pulsed laser radiation.

Another method to assess irreversible detector damages is to measure the diode characteristic that changes near the damage threshold. The breakdown voltage decreases and the dark current increases (see Fig. 2-2b). These changes can be observed as a decrease of the differential resistance of the diode.

The assessment of damage thresholds was accomplished for different detector technologies, for example, CMT, InSb and PtSi at various laser wavelengths (1.06 µm, 3.8 µm, 4.01 µm, 9.5 µm, 10.6 µm).

Dazzling:

For laser radiation intensities below the damage threshold, the mission of a sensor can be disrupted due to overexposure. The dazzling effects occurring depend on the individual sensor technology used (scanning single detector, scanning linear array, focal plane array). An example for the dazzling of scanning sensors by pulsed laser radiation (nanosecond laser pulses, wavelength: 10.6 µm) is shown in Fig. 2-3 for various pulse repetition frequencies. The two different scanning technologies can be seen clearly in the dazzling pattern.

In cooperation with TNO (The Netherlands) and DGA Maîtrise de l'information (formerly named CELAR, France) the effects of laser radiation on infrared focal plane array cameras were examined [6]. Experiments were performed with three different combinations of cameras and MWIR lasers. A CMT camera was used in combination with a DF laser as well as a frequency doubled CO_2 laser and an InSb camera was used with a PPLN-OPO laser. The details of these measurements can be found in the aforementioned reference. One findings of those experiments was that for nanosecond laser pulses a nonlinear saturation phenomena occurs. For very high pulse energies, the peak pixel value in the saturated area decreased with increasing laser power.

In order to get a better understanding of the saturation phenomena described above, experiments at much shorter timescales were performed at the Fraunhofer IOSB. Fig. 2-4 shows the detector signals of a CMT thermal imager observing the diffuse reflection of laser radiation from a rough surface. As a first step, we compared the signals produced by white light femtosecond laser pulses (plot on the right hand side) with the signals of a continuous wave laser (plot on the left hand side). For the continuous wave laser beam, the dynamic range of the 14 bit sensor is completely utilized (maximum pixel value of 16384). In the case of the femtosecond laser pulses, the sensor signal is saturated at a rather low value of about 6000.

As an explanation of this phenomenon, we suppose that ultra-short laser pulses excite all those electrons in the valence band to the conduction band whose transition energy is within the spectral width of the laser pulse. Considering only the mechanisms in the detector material without taking into account the electronics behind the detector, one can assume that the amount of charge carriers available within the timescale of the laser pulse is finite. Therefore, only a limited detector signal can be produced since no further charge carriers can be excited. We conclude that this saturation phenomenon is not to be understood in the classical sense of saturation where the detector electronics limits the signals.

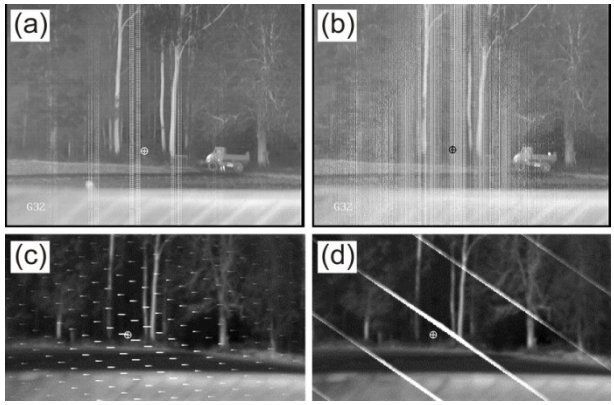

Figure 2-3.Top row: Laser dazzling effects by pulsed laser radiation on a scanning line detector: (a) Pulse repetition frequency PRF = 500 Hz, average power P = 60 mW; (b) PRF = 4 kHz, P = 1 W. Bottom row: Laser dazzling effects by pulsed laser radiation on a scanning single detector: (c) PRF = 5.1 kHz, P = 1.3 W; (d): PRF = 9.9 kHz, P = 2 W.

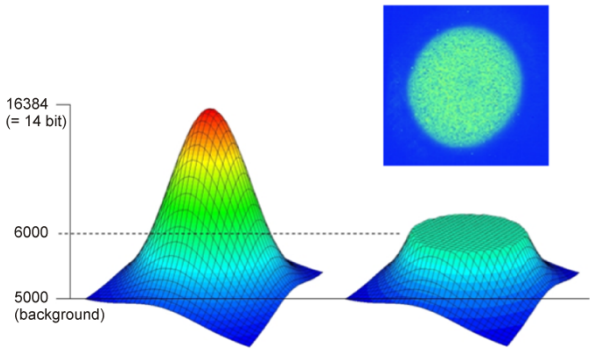

Figure 2-4. Detector signals of a CMT camera observing the diffuse reflection of laser light at a rough surface. Left: Detector signal of a cw laser beam with Gaussian intensity distribution. Right: Detector signal caused by the IR radiation of a white light femtosecond laser pulse.

2.3. Assessment of laser dazzling effects on TV cameras

In cooperation with ONERA and Institut d'Optique (both France), dazzling experiments were performed on TV CCD cameras using nanosecond laser pulses [7]. Different intensity dependent physical phenomena could be observed. To quantify these dazzling effects, pattern recognition algorithms were developed.

For the dazzling experiments, a frequency doubled Nd:YAG laser was used working at a wavelength of 532 nm. The pulse frequency could be varied from very low pulse repetition frequencies (down to 10 Hz) up to very high values (up to 100 kHz). The TV camera used in the experiments was a Sanyo VCB 3440-P which is classically used for video monitoring. It is an interlaced CCD camera with 8 bit resolution and 1/3" sensor containing 542×584 pixels. The laser beam was directed towards the camera which observed an artificial scene on a screen. A hole pierced in the screen made it possible to overlap the dazzling laser beam with the artificial scene.

The physical phenomena that gradually impaired the image of the CCD camera were observed by comparing successive images obtained for increasing values of the laser pulse energy and increasing pulse repetition frequency (PRF). Three classes of phenomena could be distinguished (see Fig. 2-5):

1. Saturation: Saturation appears with increasing laser pulse energy creating a saturated spot with intensity-dependent size.
2. Optical effects: Optical effects created in the lens of the camera considerably modified the spatial structure of the saturated spot on the camera.
3. Electronic effects: Some electronic effects appeared due to charge transfer processes and are directly related to the ratio between the PRF of the laser and the read out frequency of the camera.

At low pulse energies, the first observable effect was the saturation of pixels located at the point of incidence of the laser beam. As the energy per pulse increased, the overexposed area spread over a larger number of pixels, creating a white bright spot in the image.

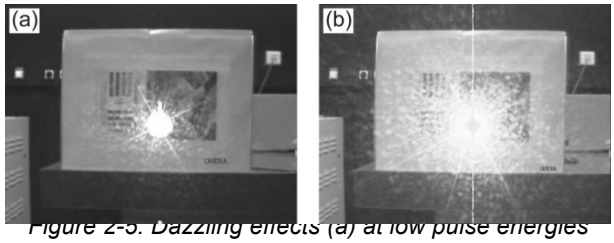

Figure 2-5: Dazzling effects (a) at low pulse energies and (b) at high pulse energies [7].

For increasing pulse energies, effects are produced which can be addressed to scattering processes in the lens and at the aperture of the camera (see Fig. 2-5a). In general, a complex light pattern appears revealing a mix of multiple reflections, diffraction and scattering in the camera lens. For even higher pulse energies, multiple concentric rings centred on the laser spot could be observed.

With sufficient high pulse energy, all pixels along the same column, which is hit by the laser spot, begin to saturate (see Fig. 2-5b). Considering that these pixels are not directly exposed to the laser beam, this saturation is related to electronic effects occurring during the charge transfer process of the CCD sensor. Depending on the pulse repetition frequency of the laser, either the complete column can be saturated (high PRF) or only a few saturated spots can be observed (low PRF).

Finally, at very high pulse energies, the pixels located at the centre of the overexposed area changed from white to grey. This behaviour is similar to that of the thermal imagers described in section 2.2.

3. PROTECTION AGAINST LASER DAMAGE

3.1. Optical power limiting

Optical power limiting goes back to the early 1960s. For example, SIEGMAN stated the "need for a limiter which can protect from overload either instrumentation or human eyes working in the vicinity of powerful optical masers, atomic explosions, and other powerful light sources" [8]. An optical power limiter (OPL) is a device showing a reduced transmittance for high input intensities, while providing high linear transmittance for low input intensities. Optical power limiting devices are based on nonlinear optical processes, among them nonlinear absorption, nonlinear refraction and in-

duced scattering are known. There is a wide range of materials showing such a nonlinear process. Beside solid-state materials, extensive investigations were made, for example, on carbon black suspension, fullerenes, carbon nanotubes, nonlinear dyes and nanoparticles. To build an OPL, these materials are either suspended in a liquid solvent or dispersed in a solid host. Solid hosts may be designed as thin films or thick samples (up to several millimetres). Several review papers on optical power limiting describing the nonlinear optical processes and suitable materials can be found in literature [9–12].

Since nonlinear optical processes are usually very weak, high laser intensities are needed to drive these processes. This circumstance has two consequences:

1. All optical power limiting devices need focusing optics where the limiting material is placed in or near the focus of the laser beam to increase the irradiance (or fluence). As an example, Fig: 3-1a shows an optical system, which was customized to fit between the folding mirrors of a tank periscope. The optics has an accessible intermediate focal plane, where a nonlinear protection filter can be placed.
2. Current optical power limiters are usually not suited as protection against laser dazzling since their activation threshold is far too high. Thus, they are intended to protect the eye or electro-optical systems only against damage by laser radiation.

The schematic response curve of an OPL is shown in Fig. 3-1b. For an ideal OPL (red curve), a constant output power is expected for input powers above the threshold. For a real OPL (green curve) the linear region of the curve passes smoothly over into the nonlinear region. Furthermore, the output power is usually not kept constant above the limiting threshold but increases with a lower slope. When the damage threshold of the OPL is reached, an optical breakdown occurs.

Generally, a high damage threshold is desired for an OPL. However, since an optical limiter device has to be located in or very close to an intermediate focal plane, optical damage will always occur somewhere above the threshold. One can make a virtue out of that fact by using the damage induced absorption and scattering to attenuate the laser radiation. In this case, the protection devices are called sacrificial elements.

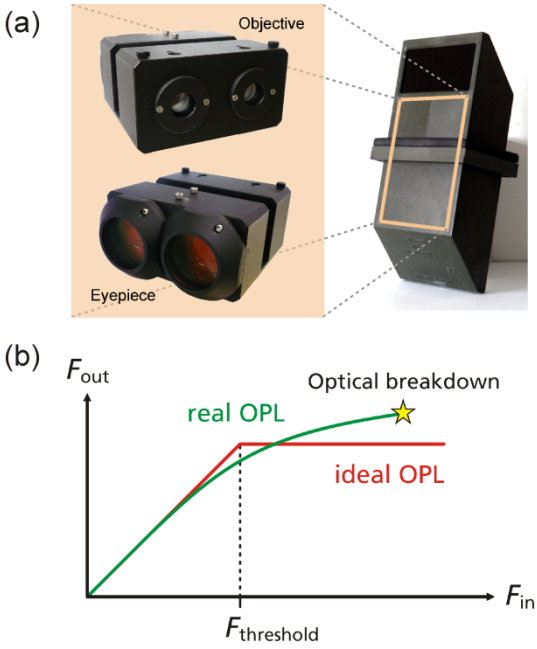

Figure 3-1. (a) Optical system with wide field of view, customized to fit between the mirrors of a tank periscope. (b) Schematic response curve of an ideal optical power limiter and a real optical power limiter.

Research on optical power limiters at the institute goes back to the early 1990s. The aim was to protect thermal imagers against damaging by laser radiation. Among various possibilities, we focused on two-photon absorption (TPA) in semiconducting materials like InSb (10.6 µm) and InAs (3.8 µm) or thermochromic effects in VO_2 (3.8 µm and 10.6 µm).

The later work comprised the evaluation of third party nonlinear laser protection filters (see [13–15]) but also the development of own devices based on nanoparticles (see [16,17]). Some of this work was performed in cooperation with the French-German Research Institute of Saint-Louis ISL (see [18–20]). Besides standard laboratory tests, the performance of nonlinear protection was also evaluated in real optical systems (see [21]).

Here, two selected examples of our work shall be presented: (a) measurements regarding optical power limiting in the infrared spectral region (section 3.2) and (b) the evaluation of the protection

performance of a sacrificial element (PMMA/Ag nanocomposite) integrated in a telescopic sight (section 3.3).

3.2. Optical power limiting in the infrared spectral region

Nonlinear effects in various materials were investigated in order to protect thermal imagers against laser radiation. In first experiments, the transmission properties of InSb for CO_2 laser radiation at 10.6 µm were measured. Fig. 3-2a shows the temporal intensity profile of a laser pulse before and after being transmitted through a 0.5 mm thick sample of InSb. The intensity modulation of the transmitted pulse can be explained by the plane parallelism of the two sample surfaces, working as an etalon.

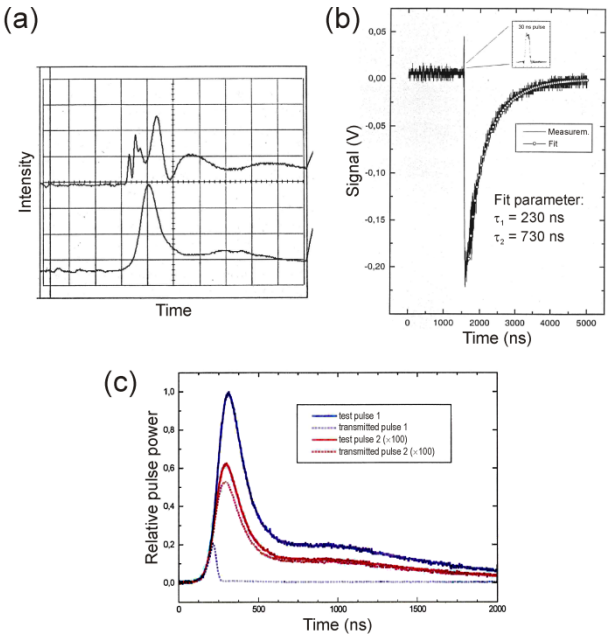

Figure 3-2. (a) Temporal intensity profile of a CO_2 laser pulse (10.6 µm) before (lower curve) and after (upper curve) the transmission through an InSb sample. (b) Measurement of the charge-carrier relaxation time of InSb at 77 K. (c)Temporal intensity profile of a CO_2 laser pulse before and after transmitting through a VO_2 sample for low (red data) and high (blue data) pulse energy.

In order to quantify the charge-carriers relaxation time of InSb, pump-probe experiments were carried out. The transmittance of the InSb sample was measured by a weak continuous wave CO_2 laser probe beam, while a short pump pulse (30 ns, cut out of the gain switch spike) changed the transmission properties of the crystal.The graph in Fig. 3-2b shows the time profile of the probe pulse for the sample cooled down to 77 K. An exponential decay with two time constants fits the data (τ_1 = 230 ns, τ_2 = 730 ns). For room temperature, the time constants are much shorter (τ_1 = 5 ns, τ_2 = 24 ns).

Another material under test was thermochromic VO_2. This material exhibits a phase transition from a transparent semi-conductive state to a reflective metallic state at a temperature of about 68 °C. Measurements of the transmittance change were carried out both with continuous wave and pulsed CO_2 laser radiation. The results for pulse durations of 200 ns are shown in Fig. 3-2c for low (red curve) and high (blue curve) pulse energies. The residual transmittance was measured to be below 5% for high pulse energies. Measurements were also performed for a laser wavelength of 3.8 µm.

3.3. Nonlinear laser protection filters in direct vision optics

The majority of measurements on optical limiting materials are usually made in laboratories. A laboratory setup is easy to establish and offers access to the focal plane to place the sample there. It also enables the researcher to optimize parameters of the setup to achieve optimal results. However, if an OPL shall be implemented in a real optical system, additional difficulties have to be considered. McGeoch and co-workers examined theoretically what has to be considered when integrating an optical limiting device into a sighting system [22]. They showed that the focal plane can move up to several millimetres due to dispersion, field curvature and temperature changes. Hence, to realize a steady protection, it has to be assured that the protection device always stays in the focal plane. Therefore, an optical limiting device for field applications most likely should be a device exhibiting a certain thickness.

At our institute, the performance of nonlinear laser protection filters was examined for different optical systems [21]. Here, we present the results of a nonlinear laser protection device (sacrificial element based on a PMMA/Ag nanocomposite) integrated in a telescopic sight (Zeiss Diavari-ZA 2.5–10×52).

The experimental setup for measuring the protection performance can be seen in Fig. 3-3. We used a frequency doubled Nd:YAG laser as laser source (Coherent Infinity, not shown in the figure, wavelength: 532 nm, pulse width: 3 ns). For the simulation of far-field conditions, the laser beam was expanded to a larger diameter by a combination of a concave lens and an off-axis parabolic mirror. A part of the laser beam was split off before entering the optical system to monitor the incident pulse energy with a reference photodiode. The input pulse energy could be changed by a set of neutral density filters.

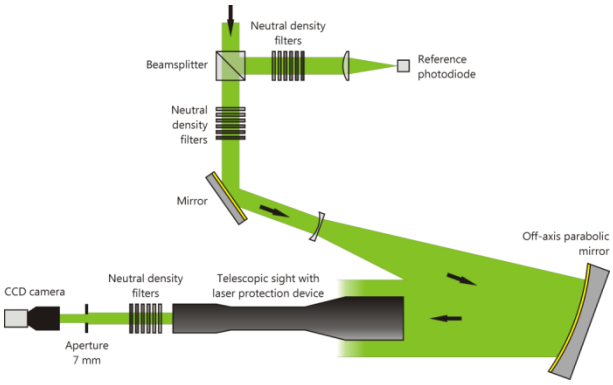

Figure 3-3. Experimental setup for the evaluation of optical limiting devices in a telescopic sight [21].

To identify the residual hazardous energy transmitted through the optical system, the focusable energy E_{foc} (or encircled energy) was measured, which is generally defined as the energy transmitted through a 1.5 mrad aperture [11]. Usually, this is realized by positioning a pinhole in the focus of a lens with appropriate focal length in front of a detector (e.g., a power meter or photodiode). For these measurements, a different method was implemented. Instead of a combination of lens, pinhole and photodiode we used a CCD camera (Kappa DX4-285 FW) with an $f = 50$ mm objective to measure the transmitted energy. After performing dark frame and flat field correction, the 1.5 mrad pinhole was simulated by integrating only the pixel signals corresponding to a field of view of 1.5 mrad.

The detection unit (CCD camera + camera lens) was protected against saturation and damage by a further set of neutral density filters. Since a telescopic sight is usually used by human observers, an aperture with diameter 7 mm was placed behind the eyepiece. The radiant energy transmitted by this aperture equals the energy that would be transmitted by the pupil of a dark-adapted eye (intraocular energy).

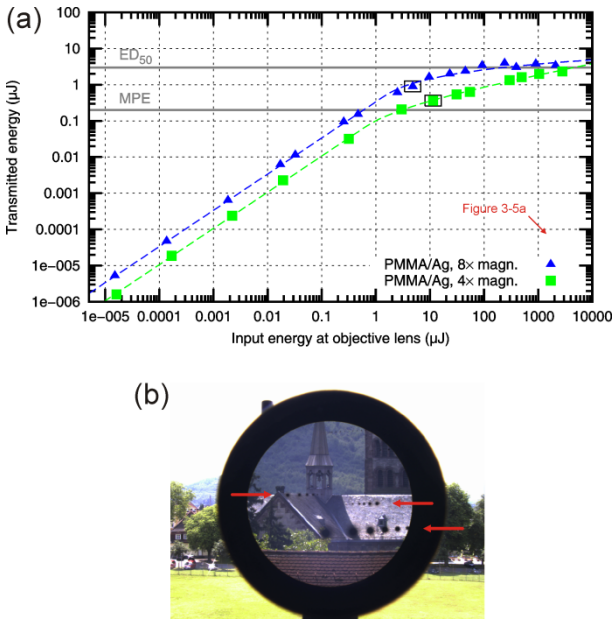

Figure 3-4. (a) Nonlinear transmittance for nanosecond laser pulses at wavelength 532 nm. (b) View through the telescopic sight (eightfold magnification) after laser fire. Adapted from [21].

The measurement results for the sacrificial element (PMMA/Ag nanocomposite) is shown in Fig. 3-4a. The plot shows the focusable energy transmitted by the combination of telescopic sight and 7 mm aperture versus the energy entering the telescopic sight. The measurements were performed at a magnification of eight and four of the telescopic sight. The horizontal lines at 0.2 J and 3.0 µJ correspond to the MPE and the ED_{50} value for retinal lesion according to reference [23], respectively. The highest transmitted energies measured were below or close to the ED_{50} value for input pulse energies of some millijoules. For fourfold magnification of the telescopic sight, the response curve of the protection filter is shifted towards lower output energies, because in this case the diameter of the transmitted laser beam is larger than for eightfold magnification. Thus, the 7 mm aperture placed behind the eyepiece blocks more radiant energy transmitted by the telescopic sight. The measurement points in each curve

where damage in the protection filter occurred for the first time are marked by black rectangles.

A view through the telescopic sight after laser fire can be seen in Fig. 3-4b for eightfold magnification of the telescopic sight. A multitude of damaged spots of various sizes is visible; some are marked by red arrows. Even though a large number of damaged spots are visible, the optics would be still usable without severe disturbance.

Advanced evaluation: In a standard test setup for optical power limiting devices, a 1.5 mrad pinhole is used to measure the focusable component E_{foc} of the transmitted energy. This value is usually compared to the point source MPE to assess the protection performance. HOLLINS states, regarding this approach, "Comparison of the 'focusable energy' E_{foc} against published ocular damage thresholds provides a basis for preliminary assessment of protection; however, proper assessment must take fuller account of the diffuse component and other issues" [11].

Since the measurement of the transmitted energy was realized with a CCD camera, the spatial intensity distribution on the CCD sensor could be used for an advanced evaluation. Fig. 3-5a shows a false colour representation of the intensity distribution at the CCD sensor for a high value of the input pulse energy. This image corresponds to the blue measurement point in Fig. 3-4a that is marked with a red arrow. Three circles (white, yellow and green) are visible in Fig. 3-5a.

The white circle corresponds to the area of a "virtual 1.5 mrad pinhole" and is centred to the maximum pixel value of the intensity distribution. We can see that the pulse energy is distributed over an area considerably larger than the area of this virtual pinhole. In a standard setup, only the fraction of energy falling into this area would be measured; whereas in reality, also a larger amount of energy would enter the eye of an observer.

To calculate the total incident energy E_{total}, the values of the pixels lying inside the yellow circle (only visible in the corners of the intensity distribution image) were integrated. Since the total incident energy is distributed over a larger area than 1.5 mrad, the extended source MPE has to be taken into account for the assessment of the protection performance. For the calculation of the extended source MPE (see [4]), the diameter of the intensity distribution was determined according to the D4σ method [24]. This diameter is indicated in Fig. 3-5a by the green circle.

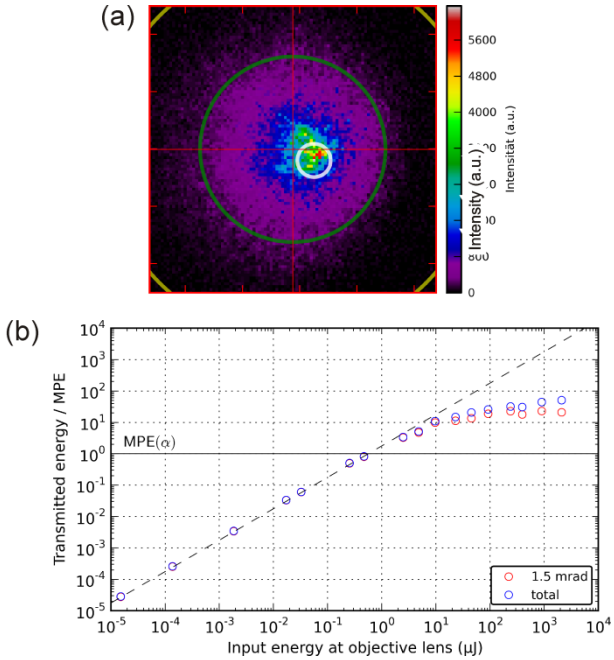

Figure 3-5. (a) False colour representation of the intensity distribution at the CCD sensor for high input pulse energy. This intensity distribution corresponds to the blue measuring value of Fig. 3-4a, which is marked with a red arrow. (b) Ratio of transmitted energy to MPE as a function of the input energy. The ratio was calculated using either the total transmitted energy (blue measuring values) or only the focusable component of the transmitted energy (red measuring values).

Fig. 3-5b shows the ratio of transmitted energy to MPE as a function of input energy. The transmitted energy was calculated either by integrating only the pixels values in the virtual pinhole (E_{foc}, red measuring values) or by integrating over the complete intensity distribution (E_{total}, blue measuring values). For the red measuring values, the point source MPE was used to calculate the ratio E_{foc} / MPE. For each blue measuring value, the diameter of the corresponding intensity distribution on the CCD sensor was calculated. This diameter was used to estimate the "individual" MPE of each blue measuring value in compliance with the laser safety regulations. Subsequently, the ratio E_{total} / MPE was calculated.

We can see from Fig. 3-5b that the use of a 1.5 mrad pinhole in a standard test setup results in an overestimation of the protection performance for higher input pulse energies.

4. PROTECTION AGAINST LASER DAZZLING

These days, an increasing threat originates from handheld laser pointers, which are obtainable with output powers in the range of 1 W and more. A large variety of different wavelengths in the visible spectral region is offered. Typically, these lasers emit continuous wave radiation, which means that active laser protection measures are a possible solution for this threat. An overview of various active laser protection techniques is given in the publication of SVENSSON and co-workers [3], among them the use of spatial light modulators (SLM). Based on this technology, an electro-optical sensor hardened against dazzling by continuous wave laser sources was developed.

The application of spatial light modulators as a protection measure against dazzling light sources was described, for example, by TOMILIN and DANILOV [25]. In previous investigations, we demonstrated successfully such an approach [26,27]. The applicability of this method was significantly improved by the implementation of wavelength multiplexing. This technique allows both spatial and spectral filtering of monochromatic light.

Wavelength multiplexing is a technique that was used by KOESTER to improve the quality of images transferred through optical fibre bundles [28]. The idea was to transmit the various wavelengths from a given object point through a number of different fibres. It was realized by placing a direct vision prism in front of the input optical system of a fiberscope, which imaged the object onto the entrance facet of the fibre bundle. Thus, the light from a given object point was spectrally broken down and then transmitted through the fibre bundle. A corresponding dispersing element at the exit end of the fibre bundle reversed the dispersion. Therefore, undesired transmission errors of the fibre bundle, for example by broken fibres and the facet structure, were reduced.

A scheme of an experimental setup combining the SLM technology with the wavelength multiplexing technique is shown in Fig. 4-1. A digital micromirror device (DMD) is used as intensity modulator. In order to be able to filter light only in localized areas of the sensor's field of view, the DMD is located at the intermediate focal plane of a 1:1 Keplerian telescope (formed by lenses L1 and L2). Before and behind the telescope, two identical dispersive elements (gratings Gr1 and Gr2) are inserted into the optical beam path to implement the wavelength multiplexing. The first grating spectrally breaks down light beams entering the setup. Each object point of a distant scene forms a wavelength spectrum at the intermediate focal plane of the telescope. The dispersion by the first grating is reversed behind the telescope by means of the second grating.

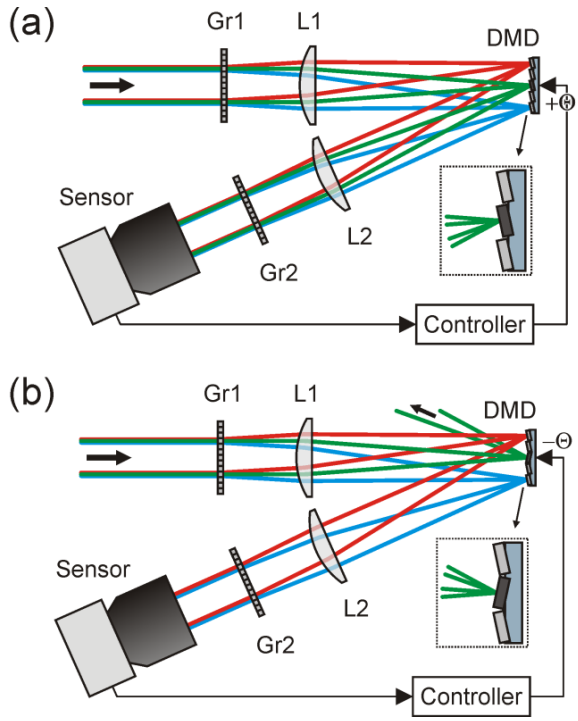

Figure 4-1. Laser dazzling protection concept using a digital micromirror device (DMD). (a) Operation mode for regular imaging. (b) Operation mode with high attenuation for dazzling light.

Usually, this setup would be operated in such a way that all light is directed towards the sensor by tilting the micromirrors completely to the +Θ-state (Fig. 4-1a). In the case of dazzling laser light arriving at the sensor (here: the green rays in the figure), the controller toggles just these micromirrors to the -Θ-state which are exposed with dazzling light (Fig. 4-1b). Thus, the dazzling light is reflected

out of the beam path, whereas all the remaining wavelengths coming from the same object point can pass the optical arrangement unaffected. Such a setup allows combined spatial and spectral filtering of monochromatic light sources and ideally suppresses only the threatening laser light, while not affecting the non-threatening radiation from the scene.

Detailed information about the optical layout with the DMD and the control loop mechanism can be found in various publications [29–32]. An earlier setup using a liquid crystal SLM in combination with direct vision prisms as dispersive elements is described in more detail in other publications [26,27].

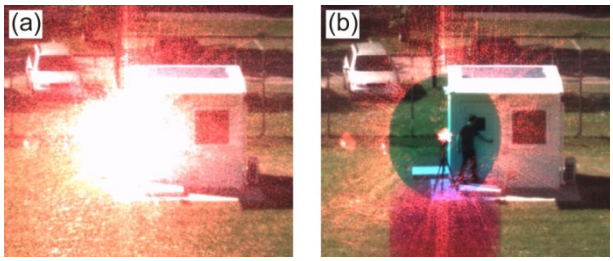

Figure 4-2. (a) Disturbed scene: Laser radiation dazzles the camera. (b) View of the scene while the filtering is switched on. As a side effect a vertically arranged colour distortion is recognizable.

The results of a field trial are shown in Fig. 4-2. A continuous wave laser (wavelength: 660 nm, output power: 2.7 mW) was placed in a distance of 73 m to the sensor. These parameters would correspond to a laser output power of 81 mW in a distance of 400 m. When the laser was switched on, a large part of the central field of view was completely dazzled (see Fig. 4-2a). As soon as the control loop of the system was activated, the dazzling laser radiation was strongly attenuated (see Fig. 4-2b). Since a band of wavelengths was extracted out of the imaging path, a colour distortion occurred, but the details in the vicinity of the laser (e.g., the person) are visible.

In the spectral region between 470 nm and 725 nm, we measured a mean attenuation of 45.4 dB for monochromatic light. The mean transmittance of the optical setup in the same wavelength range is 0.26.

5. SUMMARY

In this publication, an overview of the work on laser protection at the Fraunhofer IOSB was given. The work performed during more than 20 years comprises the analysis of laser threats as well as research on laser protection measures. As one outcome of the work, it was shown that wavelength-independent laser protection could be realized for specific application fields. One example is the hardening of direct vision optics by making use of optical power limiters. These devices are suitable to prevent (or minimize) laser damage; however, they are restricted to optical systems with intermediate focal plane. Another example presented is the hardening of electro-optical sensors against laser dazzling. Unfortunately, all non-conventional laser protection measures have their limits (e.g., maximum attenuation or transmittance losses). A solution that is capable to counter every laser threat is still far out of reach.

6. REFERENCES

1. http://kbtochmash.com/products-eng/products-eng1/products-eng1_79.html
   Last access: 2013-08-20.
2. Wong, W. W. S. (2013). *Emerging Military Technologies*, Praeger, p. 74.
3. Svensson, S., Björkert, S., Kariis, H. & Lopes, C. (2006). Countering laser pointer threats to road safety.
   Proc. SPIE **6402**, 640207.
4. *Safety of laser products – Part 1: Equipment classification and requirements* (IEC 60825-1:2007); German version EN 60825-1:2007.
5. Nakagawara, V. B., Montgomery, R. W., Dillard, A. E., McLin, L. N. & Connor, C. W. (2004). *The Effects of Laser Illumination on Operational and Visual Performance of Pilots During Final Approach*, Office of Aerospace Medicine, Federal Aviation Administration.
6. Schleijpen, R. (H.) M. A. et al. (2007). Laser dazzling of focal plane array cameras.
   Proc. SPIE **6738**, p. 67380O.
7. Durécu, A. et al. (2007). Assessment of laser-dazzling effects on TV-cameras by means of pattern recognition algorithms.
   Proc. SPIE **6738**, p. 67380J.

8. Siegman, A. E. (1962). Nonlinear optical effects: An optical power limiter.
Appl. Opt. **1**, pp- 739–744.
9. Tutt, L. W. & Boggess, T. F. (1993). A review of optical limiting mechanisms and devices using organics, fullerenes, semiconductors and other materials.
Prog. Quant. Elect. **17**, pp. 299–338.
10. Sun, Y.-P. & Riggs, J. E. (1999). Organic and inorganic optical limiting materials. From fullerenes to nanoparticles.
Int. Rev. Phys. Chem. **18**, pp. 43–90.
11. Hollins, R. C. (1999). Materials for optical limiters. *Curr. Opin. Solid St. M.* **4**, pp. 189–196.
12. Sun, Y.-P., Riggs, J. E., Henbest, K. B. & Martin, R. B. (2000). Nanomaterials as Optical Limiters.
J. Nonlin. Opt. Phys. & Mat. **9**, p. 481503.
13. Donval, A. et al. (2007). Wideband protection filter: single filter for laser damage preventing at wide wavelength range.
Proc. SPIE **6737**, p. 67370F.
14. Donval, A. et al. (2008). Novel filter providing human eye and optical sensors protection from the visible into the IR.
Proc. SPIE **6940**, p. 69400Z.
15. Ritt, G. et al. (2008). Wideband protection filter (WPF) integrated within optical systems.
Proc. SPIE **7113**, p. 71130Y.
16. Dengler, S., Ritt, G. & Eberle, B. (2009). Optical limiting performance of nanoparticles in liquid and solid media.
Proc. SPIE **7481**, p. 74810T.
17. Dengler, S., Kübel, C., Schwenke, A., Ritt, G. & Eberle, B. (2012) Near- and off-resonant optical limiting properties of gold–silver alloy nanoparticles for intense nanosecond laser pulses. *J. Opt.* **14**, p. 075203.
18. Dengler, S., Muller, O., Ritt, G. & Eberle, B. (2012). Influence of the geometric shape of silver nanoparticles on optical limiting.
Proc. SPIE **8545**, p. 854503.
19. Dengler, S., Muller, O., Straube, G., Ritt, G. & Eberle, B. (2012). Investigations of nanoparticles for optical power limiting. *Proceedings of the 5th International Symposium on Optronics in Defence and Security OPTRO 2012*.
20. Muller, O., Dengler, S., Ritt, G. & Eberle, B. (2013). Size and shape effects on the nonlinear optical behavior of silver nanoparticles for power limiters. *Appl. Opt.* **52**, pp. 139–149.
21. Ritt, G., Dengler, S. & Eberle, B. (2009). Protection of optical systems against laser radiation. *Proc. SPIE* **7481**, p. 74810U.
22. McGeoch, S. P., Thomson, I., Christie, A. & Hollins, R. C. (1999). Design considerations for using optical limiters in sighting systems. *Nonlinear Optics* **21**, pp. 491–502.
23. Gibbons, W. D. (1973). Retinal Burn Thresholds for Exposure to a Frequency-Doubled Neodymium Laser.
USAF Report SAM-TR-73-45.
24. ISO 11146-1:2005, *Lasers and laser-related equipment – Test methods for laser beam widths, divergence angles and beam propagation ratios*.
25. Tomilin, M. G. & Danilov, V. V. (2004). Optical devices based on liquid crystals for protecting an observer from blinding light sources.
Journal of Optical Technology **71**, pp. 75–83.
26. Ritt, G. & Eberle, B. (2010). Sensor protection against laser dazzling.
Proc. SPIE **7834**, p. 783404.
27. Ritt, G. & Eberle, B. (2011). Electro-optical sensor with spatial and spectral filtering capability. *Appl. Opt.* **50**, pp. 3847–3853.
28. Koester, C. J. (1968). Wavelength Multiplexing in Fiber Optics.
J. Opt. Soc. Am. **58**, pp. 63–67.
29. Ritt, G. & Eberle, B. (2011). Protection concepts for optronical sensors against laser radiation. *Proc. SPIE* **8185**, p. 81850G.
30. Ritt, G, & Eberle, B. (2012). Automatic suppression of laser dazzling effects for electro-optical sensors by a sophisticated filtering concept. *Proceedings of the 5th International Symposium on Optronics in Defence and Security OPTRO 2012*.
31. Ritt, G. & Eberle, B. (2012). Automatic Suppression of Intense Monochromatic Light in Electro-Optical Sensors.
Sensors **12**, pp. 14113–14128.
32. Ritt, G. & Eberle, B. (2012). Electro-optical sensor with automatic suppression of laser dazzling. *Proc. SPIE* **8541**, p. 85410P.